Pip5 Transduction Peptides Direct High Efficiency Oligonucleotide-mediated Dystrophin Exon Skipping in Heart and Phenotypic Correction in *mdx* Mice

HaiFang Yin[1,2], Amer F Saleh[3], Corinne Betts[1], Patrizia Camelliti[1], Yiqi Seow[1], Shirin Ashraf[1], Andrey Arzumanov[3], Suzan Hammond[1], Thomas Merritt[1], Michael J Gait[3] and Matthew JA Wood[1]

[1]Department of Physiology, Anatomy and Genetics, University of Oxford, Oxford, UK; [2]Tianjin-Oxford Joint Laboratory of Gene Therapy, Tianjin Research Centre of Basic Medical Science, Tianjin Medical University, Tianjin, China; [3]Medical Research Council Laboratory of Molecular Biology, Cambridge, UK

Induced splice modulation of pre-mRNAs shows promise to correct aberrant disease transcripts and restore functional protein and thus has therapeutic potential. Duchenne muscular dystrophy (DMD) results from mutations that disrupt the *DMD* gene open reading frame causing an absence of dystrophin protein. Antisense oligonucleotide (AO)-mediated exon skipping has been shown to restore functional dystrophin in *mdx* mice and DMD patients treated intramuscularly in two recent phase 1 clinical trials. Critical to the therapeutic success of AO-based treatment will be the ability to deliver AOs systemically to all affected tissues including the heart. Here, we report identification of a series of transduction peptides (Pip5) as AO conjugates for enhanced systemic and particularly cardiac delivery. One of the lead peptide-AO conjugates, Pip5e-AO, showed highly efficient exon skipping and dystrophin production in *mdx* mice with complete correction of the aberrant *DMD* transcript in heart, leading to >50% of the normal level of dystrophin in heart. Mechanistic studies indicated that the enhanced activity of Pip5e-phosphorodiamidate morpholino (PMO) is partly explained by more efficient nuclear delivery. Pip5 series derivatives therefore have significant potential for advancing the development of exon skipping therapies for DMD and may have application for enhanced cardiac delivery of other biotherapeutics.

Received 12 December 2010; accepted 24 March 2011; published online 19 April 2011. doi:10.1038/mt.2011.79

INTRODUCTION

Duchenne muscular dystrophy (DMD) is a severe muscle degenerative disorder resulting from mutations that disrupt the *DMD* gene open reading frame leading to the absence of functional dystrophin protein.[1,2] Antisense oligonucleotide (AO)-mediated exon skipping can restore the open reading frame of mutant *DMD* pre-mRNA transcripts[3–15] and produce truncated but partially functional dystrophin protein.[16,17] The therapeutic potential of this method has been shown in human subjects following local intramuscular AO injection in two independent clinical trials.[10,18]

DMD is a systemic disease affecting skeletal muscles, as well as heart muscle and brain. Therefore, successful AO exon-skipping therapy will depend critically on effective AO delivery to all affected tissues. Systemic delivery of 2′-O-methyl phosphorothioate and phosphorodiamidate morpholino (PMO) AOs have been shown to restore dystrophin protein expression in multiple peripheral muscle groups in dystrophin-deficient *mdx* mice but with low efficiencies even at high doses.[6,8] More recently, enhanced systemic delivery of PMO AOs has been reported via AO conjugation to positively charged, arginine-rich (Arg-rich) cell-penetrating peptides (CPPs).[13,14,19–21] All of these studies reported significant dystrophin protein restoration in multiple muscle groups at low PMO doses compared with unmodified PMO, with limited dystrophin correction in heart muscle, and improvement of the *mdx* phenotype.

Peptide-PMO conjugates therefore have high potential as novel therapeutic agents for DMD. However, recent *mdx* mouse studies have been limited to AO conjugates of a small number of Arg-rich CPPs and have yet to explore novel peptide domain design space more widely. Further, such CPPs have been generally proved to be poorly effective for enhanced delivery to critically affected tissues such as heart and brain. We previously reported preliminary studies on a novel series of transduction peptides termed Pip (PNA/PMO internalization peptide) based on mutagenesis and functional studies arising from an original R_6-Penetratin CPP.[22] In this work, the Pip2b peptide enhanced the cellular uptake of a splice-redirecting peptide nucleic acid (PNA) AO in a pLuc705 HeLa cell model and elicited exon skipping of the *DMD* gene transcript

The first two authors contributed equally to this work.

Correspondence: *Matthew JA Wood, Department of Physiology, Anatomy and Genetics, University of Oxford, South Parks Road, Oxford, OX1 3QX, UK. E-mail: matthew.wood@dpag.ox.ac.uk or Mike Gait, MRC Laboratory of Molecular Biology, Hills Road, Cambridge CB2 0QH, UK. E-mail: mgait@mrc-lmb.cam.ac.uk*

and dystrophin production following intramuscular injection of Pip2b-PNA in *mdx* mice.[22]

Here, we report the discovery and characterization of novel Pip transduction peptides with high potential for systemic PMO delivery. We identify Pip5e as showing high exon skipping efficiency and dystrophin production as a PMO conjugate in all peripheral muscles in *mdx* mice, and with the capacity for complete molecular correction in heart muscle.

RESULTS

To explore the therapeutic potential of Pip series peptides for directing *in vivo* systemic AO delivery and dystrophin splice correction, we developed and characterized further novel peptides and evaluated their potential following intramuscular and systemic intravenous injection in *mdx* mice.

Pip series peptide development and identification of Pip5e

Pip2b conjugated to a 20-mer PNA AO targeting at murine DMD exon 23 (Pip2b-PNA) had previously shown significantly higher exon skipping activity in differentiated *mdx* mouse myotubes and approximately threefold increased number of dystrophin-positive fibers when injected into the tibialis anterior muscle of the *mdx* mouse compared to $(RAhxR)_4$-PNA (R-PNA).[22] After several rounds of sequence modifications including simplification and shortening, PNA conjugations and cell assays, we identified Pip5e (**Figure 1a**), which contains a central ILFQY hydrophobic motif flanked on each side by Arg-rich domains containing only arginine, aminohexyl (X) and β-alanine (B) residues. In differentiated *mdx* mouse myotubes, Pip5e-PNA induced very similar levels of exon skipping at 1 and 2 µmol/l concentrations in the absence of any transfection agent compared to Pip2b-PNA and both showed significantly higher exon skipping activity than R-PNA (**Figure 1b**).

Since the leading charge-neutral AO cargo currently undergoing clinical trials is PMO[6,18] with reports of substantially enhanced effectiveness of R-PMO and B-PMO conjugates by systemic delivery into *mdx* mice compared to naked PMO,[13,14,19–21] we compared Pip5e-PNA and Pip5e-PMO conjugates in the *mdx* mouse model. A simplified conjugation procedure was developed (**Figure 1a**) followed by single step high-performance liquid chromatography purification (see **Supplementary Materials and Methods** and **Supplementary Figure S1**). In differentiated *mdx* mouse myotubes, Pip5e-PMO showed approximately twofold higher exon skipping activity compared to Pip5e-PNA (**Figure 1c**). Although

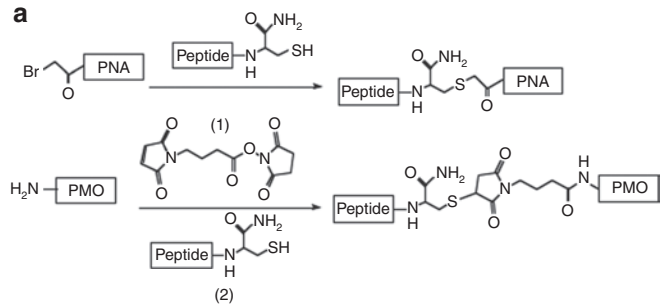

Name	Peptide sequence	Length
R	RXRRXRRXRRXRXB	14
B	RXRRBRRXRRBRXB	14
Pip2b	RXRRXRRXR-IHILFQN-dRRMKWHKB	24
Pip5e	RXRRBRRXR-ILFQY-RXRBRXRB	22
Pip5f	RXRRBRRXR-ILFQY-RXRXRXRB	22
Pip5h	RXRRXR-ILFQY-RXRRXR	17
Pip5j	RBRRXRRBR-ILFQY-RBRXRBRB	22
Pip5k	RBRRXRRBR-ILFQY-RXRBRXRB	22
Pip5l	RBRRXRRBR-ILFQY-RXRRXRB	21
Pip5m	RBRRXRRBR-ILFQY-RXRBRXB	21
Pip5n	RXRRBRRXR-ILFQY-RXRRXRB	21
Pip5o	RXRRBRRXR-ILFQY-RXRBRXB	21

PNA = GGCCAAACCTCGGCTTACCT
PMO = GGCCAAACCTCGGCTTACCTGAAAT

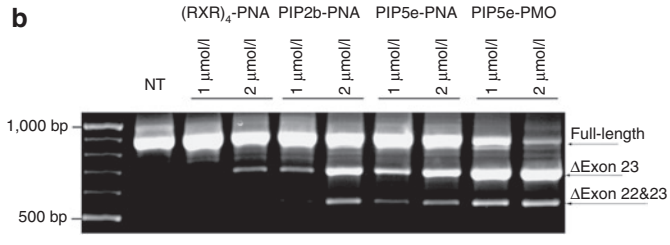

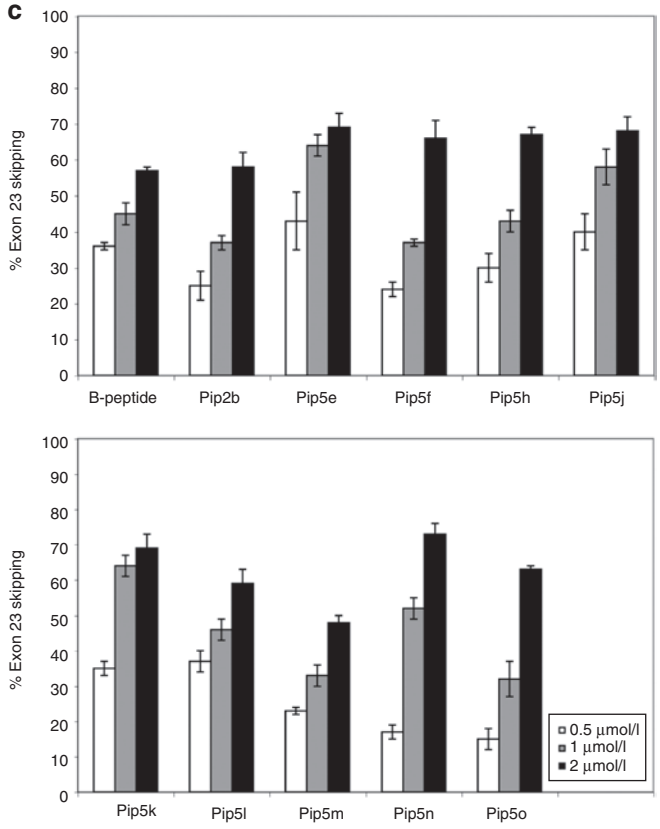

Figure 1 Synthesis and cellular activity of Pip5-phosphorodiamidate morpholino (PMO) conjugates. (**a**) Schemes showing the conjugation chemistries for synthesis of peptide-peptide nucleic acid (PNA) via thioether linkage (top) and peptide-PMO via thiol-maleimide linkage (middle). The names and sequences of the peptides used in this study as well as the sequences of the PNA and PMO antisense oligonucleotide (AO) are shown below. (**b**) Levels of exon skipping by $(RXR)_4$-PNA, Pip2b-PNA, Pip5e-PNA, and Pip5e-PMO at 1.0 and 2.0 µmol/l concentrations following incubation with *mdx* mouse myotubes in the absence of transfection agent and reverse transcriptase (RT)-PCR analysis. (**c**) Percentage of exon skipping for PMO conjugates of B, Pip2b, and Pip5e to Pip5o at 0.5, 1.0, and 2.0 µmol/l.

PMO is a 25-mer, compared to the 20-mer of PNA AO, we found that Pip2b-PNA25 (25-mer with the same sequence as PMO) did not have higher activity than Pip2b-PNA (20-mer).[23] Therefore, higher exon skipping activity is unlikely not only due to the longer length of PMO compared to PNA, but also rather due to the use of PMO, rather than PNA, as cargo when Pip-conjugated.

We then synthesized a range of PMO conjugates with analogues of Pip5e (Pip5f to Pip5o) having variations in the numbers and placement of X, B, and Arg residues in the flanking Arg-rich sections (**Figure 1a**). Pip5-PMO conjugates were evaluated at 0.5, 1, and 2 µmol/l concentrations in differentiated *mdx* myotubes (**Figure 1c**). Considering the results broadly across all three concentrations, Pip5e, Pip5j, Pip5k, and Pip5n showed higher exon skipping than the B-PMO control (B is a variant of R where two X residues are replaced by B residues, **Figure 1a**). By contrast, Pip5f-PMO, Pip5h-PMO, Pip5m-PMO, and Pip5o-PMO were slightly less active. Unexpectedly, Pip2b, previously selected as being several-fold higher in activity as a PNA conjugate compared to R-PNA,[22] also showed slightly less activity when conjugated to PMO than B-PMO.

Intramuscular evaluation of novel Pip5 series Pip-PMO conjugates

Pip5-PMO conjugates (Pip5e, 5f, 5h, 5j, 5k, 5l, 5m, 5n, 5o) were next evaluated for *in vivo* activity by intramuscular injection into the tibialis anterior muscles of *mdx* mice (**Figure 2**). Dystrophin production was analyzed by immunohistochemistry to detect *de novo* dystrophin protein expression (**Figure 2a**). A number of Pip5-PMO conjugates demonstrated higher exon skipping activity than previously studied B-PMO and Pip2b-PMO, with the highest activity shown by Pip5e, 5j, and 5n conjugates and confirmed by quantification of dystrophin-positive fiber numbers (**Figure 2b**). The splice correcting activity of Pip5-PMO compounds was confirmed by reverse transcriptase (RT)-PCR (**Figure 2c**) and western blot studies (**Figure 2d**), showing high efficiency exon skipping and protein restoration by a number of Pip5 conjugates.

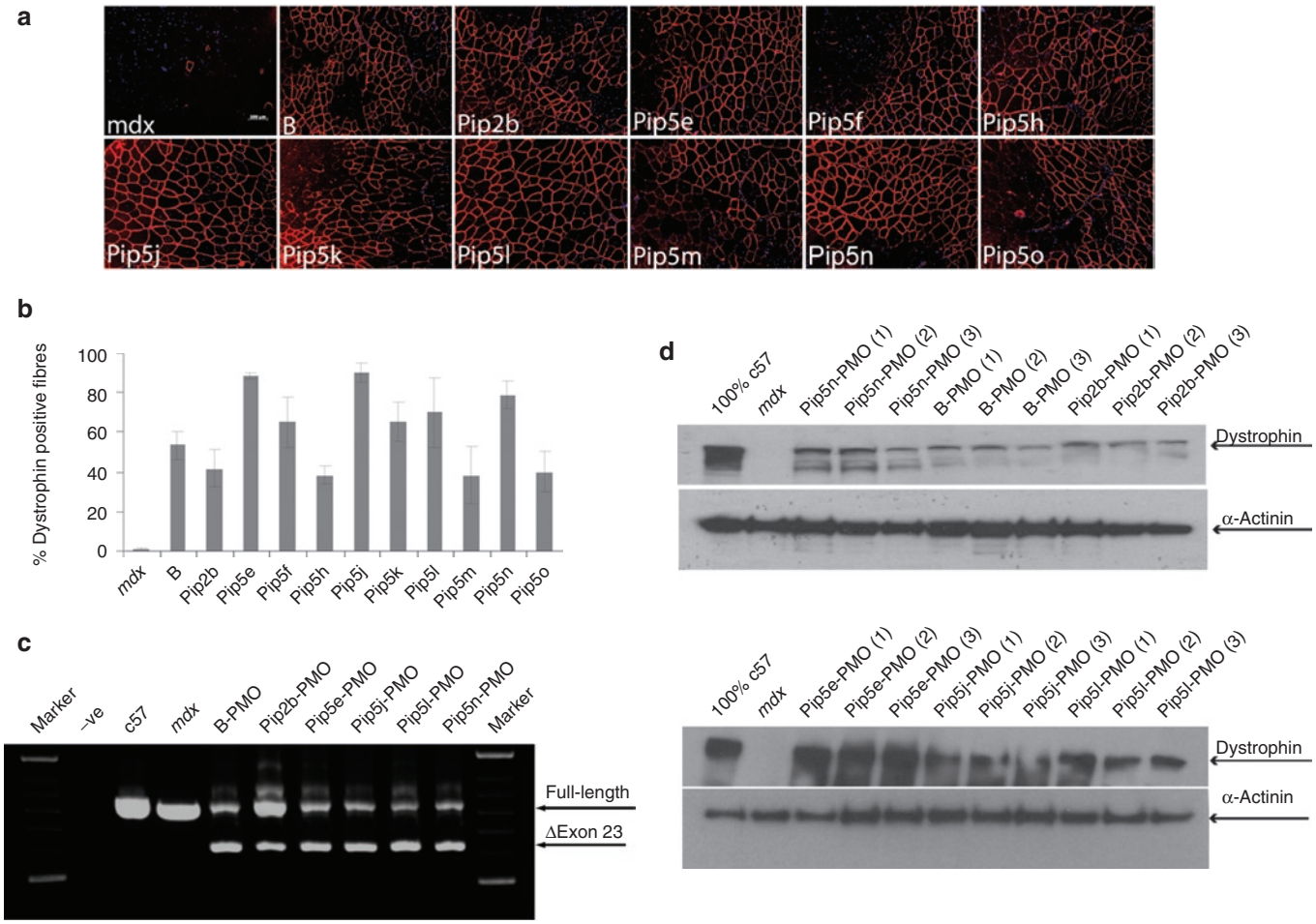

Figure 2 Screen of novel Pip5-phosphorodiamidate morpholino (PMO) conjugates following intramuscular administration in *mdx* mice. Dystrophin expression following single intramuscular injection into tibialis anterior (TA) at 5 µg doses in adult *mdx* mice. (**a**) Immunohistochemical staining for dystrophin in *mdx* TA muscles following 5 µg injection of peptide-PMO conjugates (bar = 100 µm). (**b**) Quantitative evaluation of total dystrophin-positive fibers in treated TA muscles 2 weeks after injection. The data are presented as percent of dystrophin-positive fibers. (**c**) Reverse transcriptase (RT)-PCR for detecting exon skipping efficiency at the RNA level, which is shown by shorter exon-skipped bands (indicated by the numbered Δexon 23–exon 23 skipped). (**d**) Western blot analysis of TA muscles from *mdx* mice treated with different peptide-PMO conjugates. Total protein was extracted from TA muscles of treated *mdx* mice 2 weeks after injection. Ten micrograms of total protein from *C57BL6*, untreated *mdx* mice TA muscles and treated muscle samples was loaded. α-Actinin was used as the loading control.

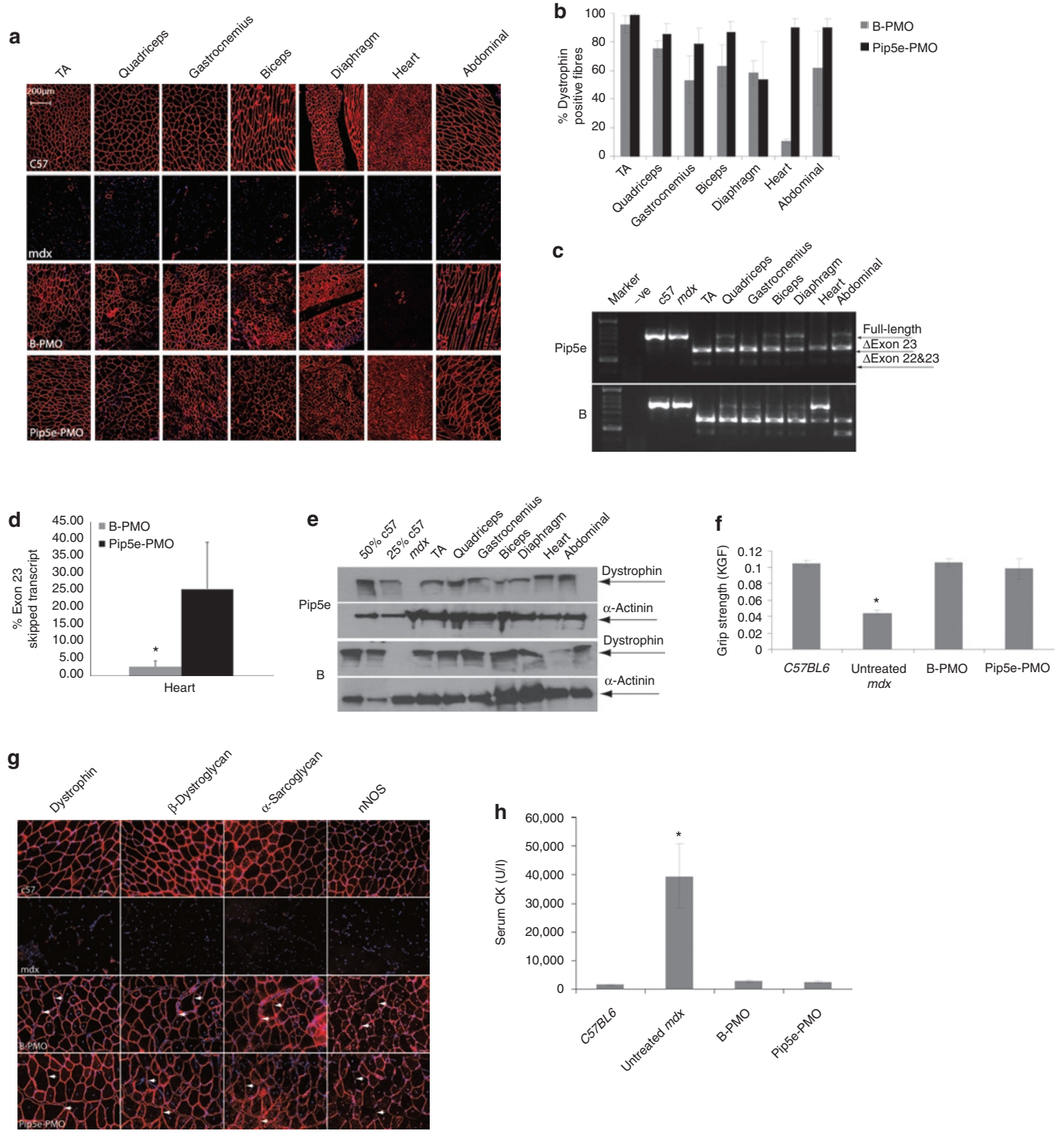

Figure 3 Systemic evaluation of Pip5e-phosphorodiamidate morpholino (PMO) in adult *mdx* mice. Functional restoration of dystrophin in *mdx* mice following single intravenous injection of 25 mg/kg Pip5e-PMO. (**a**) Immunohistochemistry for dystrophin in body-wide muscles of adult *mdx* mice 2 weeks after treatment with either Pip5e-PMO (bottom panel) or B-PMO (third panel), and normal *C57BL6* (top panel) and untreated *mdx* mice (second panel) are shown. TA represents tibialis anterior (bar = 200 μm). (**b**) Quantitative evaluation of total dystrophin-positive fibers in all tested muscles. (**c**) Reverse transcriptase (RT)-PCR to detect the dystrophin exon skipping products in various treated *mdx* muscle groups; unskipped or deleted for exon 23 or exon 22 and 23 as indicated in the boxes. (**d**) Quantative PCR results for exon skipping in heart treated with Pip5e-PMO and B-PMO at the dose of 25 mg/kg in adult *mdx* mice. (**e**) Western blot to detect dystrophin protein in treated *mdx* mice with Pip5e- and B-PMO compared with *C57BL6* and untreated *mdx* control mice. α-Actinin was used as the loading control. (**f**) Muscle function was assessed to determine the physical improvement of peptide-PMO conjugates treated *mdx* mice compared with *C57BL6* and untreated *mdx* mice. Data show significant functional improvement in treated *mdx* mice compared to untreated age-matched control mice (*$P < 0.005$). (**g**) Expression of the dystrophin-associated protein complex components in *mdx* mice to assess dystrophin function and recovery of normal myoarchitecture. (**h**) Serum creatine kinase (CK) levels. Data show a significant fall in *mdx* mice treated with peptide-PMO conjugates compared with untreated age-matched *mdx* controls ($n = 6$, *$P < 0.05$).

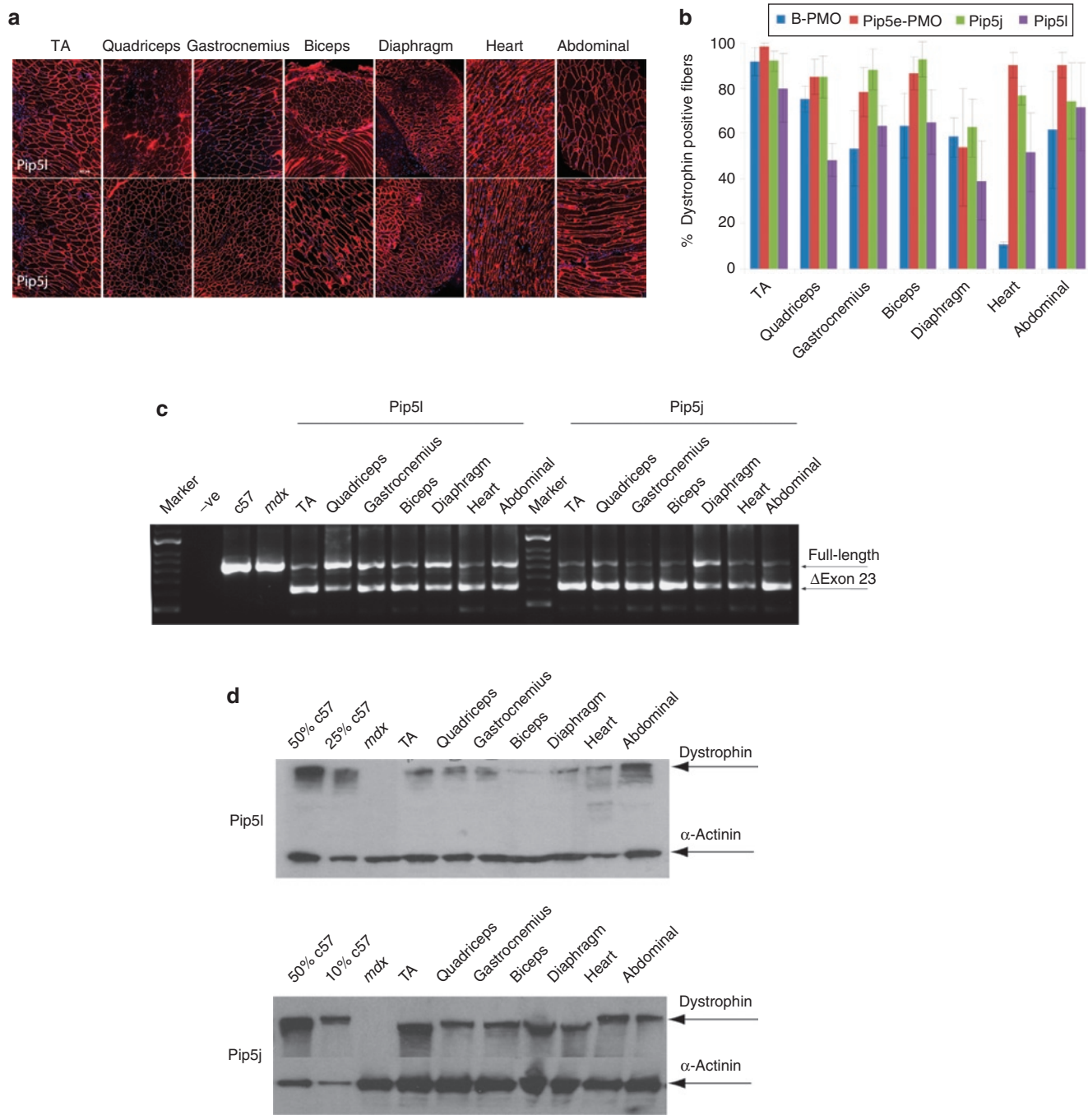

Figure 4 Investigation of other Pip5 peptides by systemic intravenous injection in *mdx* mice at the 25 mg/kg dose. Restoration of dystrophin expression in body-wide muscles following single intravenous injection of Pip5j and Pip5l-phosphorodiamidate morpholino (PMO) at 25 mg/kg dose. (**a**) Immunohistochemistry for dystrophin induction in body-wide muscles of adult *mdx* mice 2 weeks after one single intravenous injection of either Pip5l-PMO (bottom panel) or pip5j-PMO (top panel) at the 25 mg/kg dose (bar = 200 µm). (**b**) Quantitative evaluation of total dystrophin-positive fibers in all tested muscles. The data are presented as percent of dystrophin-positive fibers, which showed the enhanced exon skipping activity observed in all tested Pip5 peptides. (**c**) Reverse transcriptase-PCR to detect the dystrophin exon skipping products in various treated *mdx* muscle groups as shown; unskipped or deleted for exon 23 or exon 22 and 23 as indicated in the boxes. (**d**) Western blot to detect dystrophin protein in the indicated muscle groups from treated *mdx* mice compared with *C57BL6* and untreated *mdx* control mice. Data shows up to 25% dystrophin expression in heart treated with Pip5e-PMO. Equal loading of 10 µg protein is shown for each sample except for *C57BL6* control lane where 1 µg of protein was loaded. α-Actinin expression was detected as the loading control.

Pip5e directs efficient systemic dystrophin protein restoration with complete cardiac splice correction

To explore the potential of Pip5-PMO for directing systemic dystrophin splice correction, we selected Pip5e for further study on the basis of the highest level activity of Pip5e-PMO following intramuscular injection in *mdx* mice (**Figure 2**). A single intravenous injection of 25 mg/kg of Pip5e-PMO was carried out in adult *mdx* mice and the levels of dystrophin production and

exon skipping analyzed in peripheral muscles and heart muscle 2 weeks postinjection (**Figure 3**). High-level dystrophin expression was detected in all peripheral muscles studied by immunohistochemistry (**Figure 3a**), with notably higher levels than in untreated or B-PMO treated *mdx* mice. Of particular note was the exceptionally high level of dystrophin protein expression in heart muscle. The numbers of dystrophin-positive fibers in the various peripheral muscle groups, including diaphragm, and heart muscle were quantified (**Figure 3b**), which confirmed the high level of dystrophin restoration following systemic treatment with Pip5e-PMO. Excess of 80% dystrophin-positive fibers were detected in all muscle groups with Pip5e-PMO excluding diaphragm where levels were slightly lower. The greatest increase in dystrophin production was detected in heart muscle, where Pip5e-PMO gave virtually complete cardiac muscle correction with >90% of dystrophin-positive fibers, whereas B-PMO was poorly active under single dose conditions. Correction of the aberrant dystrophin transcript was demonstrated by RT-PCR analysis (**Figure 3c,d**), which confirmed the high activity of Pip5e-PMO in all tissues particularly in heart, where full-length uncorrected transcript containing exon 23 was barely detectable. The efficient restoration of dystrophin protein in heart was confirmed by western blot analysis (**Figure 3e**), which showed >50% of normal levels of dystrophin protein following single dose Pip5e-PMO administration.

Functional and phenotypic correction of the *mdx* mouse following a single intravenous administration of Pip5e-PMO

To determine whether a single intravenous dose of Pip5e-PMO at 25 mg/kg could correct the *mdx* mouse phenotype, functional and serum biochemical assays were carried out (**Figure 3**). Grip strength analysis was used to study to what extent *mdx* muscle function was restored following Pip5e-PMO treatment (**Figure 3f**). This demonstrated significant improvement in *mdx* muscle strength 2 weeks following a single Pip5e-PMO administration compared with untreated mice, to levels similar to that found in wild-type *C57BL6* mice. High efficiency dystrophin protein restoration with Pip5e-PMO also resulted in efficient sarcolemmal relocalization of components of the dystrophin-associated protein complex—β-dystroglycan, α-sarcoglycan, and neuronal nitric oxide synthase—that fail to localize correctly in the absence of dystrophin protein[24,25] (**Figure 3g**). Dystrophin and dystrophin-associated protein complex molecular correction with Pip5e-PMO treatment also resulted in a significant decline in serum creatine kinase levels to within the normal range found in wild-type mice[26] (**Figure 3h**), indicating restored muscle membrane integrity. Further, following single intravenous treatment with Pip5e-PMO no evidence was found to indicate organ or immune toxicity. Serum liver function assays, liver and renal histology, and assays of the numbers of infiltrating lymphocytic, macrophage and neutrophil cells were all within the normal range (**Supplementary Figure S2a–c**).

The high systemic and cardiac activity of Pip5e-PMO was found to be retained at lower single doses of 18.75 mg/kg (**Supplementary Figure S3**) and 12.5 mg/kg in adult *mdx* mice (**Supplementary Figure S4**). Further, the lower 18.75 mg/kg systemic intravenous dose was applied to 6-month-old *mdx* mice with similar results to those found in young adult *mdx* mice with no diminution in effect observed (**Supplementary Figure S3**).

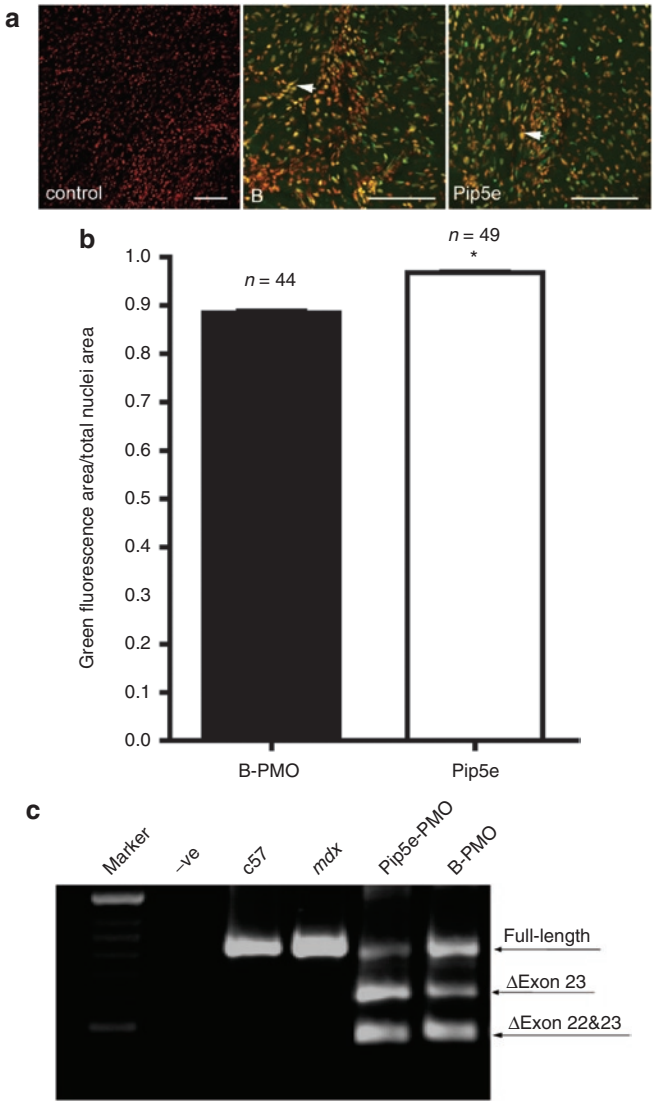

Figure 5 Cellular uptake of labeled Pip5e-phosphorodiamidate morpholino (PMO) and B-PMO in live heart slices. (**a**) Multiple two-photon microscopy images of living heart slices transfected with Hoechst alone for the nuclear staining (red, left panel), Hoechst and fluorescein isothiocyanate (FITC)-labeled B-PMO (red/green, center panel), or Hoechst and FITC-labeled Pip5e-PMO (red/green, right panel); bar = 100 µm. The arrow shows the colocalization of labeled compounds with nuclei. (**b**) Quantitative analysis of multiple photon images shows higher Pip5e-PMO nuclear uptake than B-PMO in live heart slices, suggesting that Pip5e deliver higher levels of PMO cargo to the cardiomyocyte nuclei. Y axis denotes the ratio of the nuclei area filled with FITC-labeled peptide-PMO conjugates to total nuclei area measured. 97± 0.3% of total nuclei area was filled with labeled Pip5e-PMO; and 88 ± 0.6% of total nuclei area was filled with B-PMO (*****$P < 0.0001$ *t*-test). In the graph, $n = 44$ (B-PMO) and $n = 49$ (Pip5e-PMO) means the number of images collected from six slices, which were obtained from three animals. (**c**) Reverse transcriptase-PCR to detect levels of dystrophin exon skipping in *mdx* heart slices treated with labeled Pip5e-PMO and B-PMO at the concentration of 2 µmol/l, which is shown by shorter exon-skipped bands (indicated by the numbered Δexon 23–exon 23 skipped).

Other Pip5 series peptides show enhanced heart activity which can be attributed to increased nuclear PMO delivery in cardiomyocytes

All Pip5 series peptides analyzed as Pip-PMO conjugates contain a unique 5 amino acid hydrophobic core domain IFLQY (**Figure 1a**). Therefore, we investigated whether other Pip5 peptides were also capable of conferring efficient systemic PMO exon skipping with high activity in heart. We evaluated two further Pip5 peptides systemically as Pip-PMO conjugates—Pip5l-PMO and Pip5j-PMO. Both were selected on the basis of their high activity in the intramuscular *mdx* screen, comparable to that found for Pip5e (**Figure 2**). Following single 25 mg/kg intravenous injections of Pip5l- and Pip5j-PMO in adult *mdx* mice, both compounds showed a similar systemic activity profile to that of Pip5e-PMO. Both conjugates conferred higher levels of exon skipping with high numbers of dystrophin-positive fibers detectable in heart tissue compared to B-PMO. The level of dystrophin protein restored also indicated the high heart activities of these two additional Pip5-PMO compounds (**Figures 4a–d**). Thus, Pip5-PMO compounds as a class have the capacity for high exon skipping activity particularly in heart. In the absence of the ILFQY domain, such as is found in B-PMO, substantially lower systemic exon skipping activity is detectable with only weak activity in heart under single dose conditions.

We hypothesized that a possible mechanism underlying the enhanced heart exon skipping activity observed with Pip5-PMO compounds over B-PMO might be due to higher levels of intracellular and nuclear delivery of the PMO cargo in cardiomyocytes. To test this, we developed an *in vitro* heart slice model in which 250 µm live slices of *mdx* mouse heart tissue were incubated in physiological medium. A number of different concentrations of fluorescently labeled Pip5e-PMO and B-PMO compounds were tested and at 2 µmol/l the intracellular and nuclear localization of these labeled compounds could be clearly visualized by two-photon microscopy and the efficiency of nuclear localization quantified with Image J. Quantitative analysis in multiple heart slices revealed a small but statistically significant ability of Pip5e to deliver higher levels of PMO cargo to the nuclear compartment (**Figure 5a,b**). Moreover, this increased nuclear delivery resulted in significantly higher levels of dystrophin exon skipping in *mdx* heart slices as detected by RT-PCR (**Figure 5c**).

DISCUSSION

AO-mediated splice correction has significant therapeutic potential for DMD.[10,18] A critical challenge in the development of this therapy is the discovery of methods for high efficiency systemic exon skipping and dystrophin restoration, including in heart. Following earlier studies that identified Pip2 series peptides as improved CPPs for splicing redirection of PNA AOs,[21] shorter and simpler Pip5 series peptides were developed with high activity in *mdx* mouse myotubes (**Figure 1**). An intramuscular screen of Pip5-PMO conjugates in *mdx* mice identified several with high exon skipping and dystrophin production *in vivo*, with Pip5e having the highest activity (**Figure 2**). Subsequent systemic intravenous administration of Pip5e-PMO showed high efficiency splice correction and restoration of dystrophin expression in multiple muscle groups in *mdx* mice, particularly for the first time in heart, where compared with a standard peptide-PMO known as B-PMO, complete splice correction was found and dystrophin protein restored to levels >50% of normal (**Figure 3**). The high systemic and cardiac activity of Pip5e-PMO was retained at lower doses and in older *mdx* mice. The notably high cardiac activity of Pip peptides was a class effect, with other Pip5 peptides incorporating the unique central hydrophobic ILFQY domain also having high systemic and heart exon skipping activity. The mechanism underlying the high Pip5-PMO exon skipping activity in heart was related to enhanced nuclear PMO delivery in cardiomyocytes.

Transduction or CPPs have powerful capacity for enhanced intracellular delivery of a variety of cargoes including AOs. Pip series CPPs were developed following structure and activity studies arising from an R6-Penetratin peptide, defining a relatively unoptimized 24mer lead peptide Pip2b.[22] Following iterative structure/function assays and reduction in length, the unique Pip5 series of peptides was identified, characterized by a central ILFQY hydrophobic region and flanked by Arg-rich domains. This arrangement of cationic and hydrophobic domains is unique among CPPs. Whereas the outer Arg-rich regions are very similar to the B peptide, a control in our studies, the central ILFQY sequence is a double mutant of IWFQN, a short section of Penetratin from which the Pip series was derived.[22] Further studies are in progress to define the role of this unique region.

The ability of Arg-rich peptides to enhance the systemic activity of exon skipping charge-neutral oligonucleotides has been shown in recent studies.[13,14,19–21] B-PMO is representative of this class of peptide-PMO compounds which all show the capacity for significant systemic dystrophin protein restoration but with only limited activity in heart. In the current study, Pip5e-PMO activity exceeded that of B-PMO in all peripheral muscle tissues with dramatically increased activity in heart muscle. Following a single 25 mg/kg intravenous dose, Pip5e-PMO corrected all detectable aberrant full-length *mdx* transcript in heart in an RT-PCR assay suggesting that delivery had achieved saturation. This led to dystrophin protein being detectable in 90–100% of fibers within the heart. Such dramatically high exon skipping levels in heart have not been reported previously with single dose peptide-PMO compounds. For example, Wu *et al.* administered six doses of peptide-PMO at 30 mg/kg to *mdx* mice to achieve dystrophin exon skipping at 72% of normal levels in heart,[20] and we therefore estimate that Pip5e-PMO will be likely to enhance heart exon skipping activity significantly over other peptide-PMO compounds such as B-PMO, even at repeated doses. Given that a high proportion of DMD patients develop cardiomyopathy which is a major cause of death, a dramatically improved ability to treat heart muscle and restore dystrophin protein will be of clinical importance. Moreover, a number of other neuromuscular disorders with cardiac phenotypes (e.g., myotonic dystrophy type I)[27,28] and primary cardiac disorders may be amenable to therapy with AOs that are efficiently delivered to heart tissue.

While methods to achieve efficient systemic exon skipping in DMD models have improved in recent years, the ability to achieve high efficiency in heart has been a major hurdle. The activity of systemically delivered 2′-O-methyl phosphorothioate and PMO AOs (the leading chemistries currently in clinical trial) is relatively poor but can be improved with the use of high

repeat doses, but even under these conditions heart activity is negligible.[6,8] Moreover, a recent report has indicated that at single systemic PMO doses of up to 3 g/kg dystrophin exon 23 was only skipped at 30% of the normal levels seen in the heart.[29] Even first generation peptide-PMO compounds, such as B-PMO, while significantly improving systemic exon skipping activity have poor cardiac activity at low single doses. This differential resistance of heart tissue to AO exon skipping compared with skeletal muscle tissue has been attributed to a leaky skeletal muscle sarcolemma in dystrophic muscle and a less permeable vascular barrier within heart.[30] The enhanced Pip5e-PMO exon skipping activity in this study suggests that Pip5 series peptides can overcome these barriers to effective heart PMO delivery. Moreover, their capacity for such activity appears to be related to the presence of the central hydrophobic ILFQY core domain within all Pip5 series peptides, given that Pip5j and Pip5l demonstrate similar activities, whereas B lacking this core domain shows less activity in heart than Pip peptides as shown in **Figures 3–5** and **Supplementary Figures S3 and S4**. Our live heart studies suggest that in addition to overcoming vascular and other barriers to cardiac delivery, Pip5e has an enhanced ability for nuclear delivery of its PMO cargo into cardiomyocytes, a biological property of potential importance for the delivery of splicing modulating AOs (**Figure 5**). Mutation studies are now in progress to identify the role of the ILFQY motif in enhanced heart delivery, to understand the mechanistic basis of Pip5 series activity in detail and to enhance further their beneficial delivery properties for the development of AO therapeutics for DMD and related disorders.

MATERIALS AND METHODS

Animals. Two-month and 6-month-old *mdx* mice were used in all experiments (6 mice each in the test and control groups) unless otherwise stated. The experiments were carried out in the Animal unit, Department of Physiology, Anatomy, and Genetics, University of Oxford, Oxford according to procedures authorized by the UK Home Office. Mice were killed by CO_2 inhalation at desired time points, and muscles and other tissues were snap-frozen in liquid nitrogen-cooled isopentane and stored at −80 °C.

Exon skipping in mdx mouse myotubes. H2K *mdx* myotubes were prepared and incubated with peptide-PNA and peptide-PMO conjugates in the absence of any transfection agent by the methods described previously,[21] but with minor variations (see **Supplementary Materials and Methods**). The primer sequences for the nested RT-PCR were as previously reported.[13,14] The products were examined by electrophoresis on a 2% agarose gel.

Intramuscular and systemic injections of peptide-PMO conjugates. Five micrograms of peptide-PMO conjugates in 40 µl saline buffer were injected into tibialis anterior muscles for intramuscular experiments. Various amounts of peptide-PMO conjugate in 80 µl saline buffer were injected into tail vein of *mdx* mice at the final dose of 25, 18.75, and 12.5 mg/kg, respectively. A detailed injection schedule was listed in **Table 1**.

Immunohistochemistry and histology. Series of 8 µm sections were examined for dystrophin expression and dystrophin-associated protein complex with a series of polyclonal antibodies and monoclonal antibodies as described.[13] $CD3^+$ T lymphocytes were identified with rat polyclonal[31] and detected by goat-anti-rat IgGs Alexa 594 secondary antibody (Invitrogen, Carlsbad, CA). For macrophage and neutrophil staining, polyclonal rabbit and rat primary antibodies from Abcam were used, respectively (Abcam, Cambridge, UK), and detected by goat-anti-rabbit and goat-anti-rat IgGs Alexa 594 secondary antibody (Invitrogen). Routine hematoxylin and eosin staining was used to examine overall liver and kidney morphology. For dystrophin-positive fiber counting, the maximum number of dystrophin-positive fibers in one section was counted using the Zeiss AxioVision fluorescence microscope and the muscle fibers were defined as dystrophin-positive when more than two-third of the single fiber showed continuous staining.

Protein extraction and western blot. Protein extraction and western blot were carried out as previously described.[13] Various amounts of protein from normal *C57BL6* mice as a positive control and corresponding amounts of protein from muscles of treated or untreated *mdx* mice were used. α-Actinin was used as loading control. The membrane was probed with DYS1 (NovoCastra, Newcastle Upon Tyne, UK) for the detection of dystrophin protein. The bound primary antibody was detected by horseradish peroxidise-conjugated rabbit anti-mouse IgGs and the ECL Western Blotting Analysis system (Amersham Pharmacia Biosciences, Buckinghamshire, UK). The intensity of the bands obtained from treated *mdx* muscles was measured by Image J software; the quantification is based on band intensity and area, and is compared with that from normal muscles of *C57BL6* mice.

Functional grip strength analysis. Treated and control mice were tested using a commercial grip strength monitor (Chatillon, West Sussex, UK). Each mouse was held 2 cm from the base of the tail, allowed to grip a protruding metal triangle bar attached to the apparatus with their forepaws, and pulled gently until they released their grip. The force exerted was recorded and five sequential tests were carried out for each mouse, averaged at 30 seconds apart.

Clinical biochemistry. Serum and plasma were taken from the mouse jugular vein immediately after the killing by CO_2 inhalation. Analysis of serum creatine kinase, aspartate aminotransferase, alanine aminotransferase, urea and creatinine levels was carried out by the clinical pathology laboratory (Mary Lyon Centre, Medical Research Council, Harwell, Oxfordshire, UK).

Heart slices preparation and treatment with peptide-PMO conjugates. Live heart tissue slices were prepared from the left ventricle of 4–6-months-old *mdx* mice.[32] In brief, hearts were rapidly excised, ventricular tissue blocks were dissected and mounted onto the specimen holder of a high precision vibratome (7,000 smz; Campden Instruments, Leicester, UK), in ice-cold Tyrode solution. Slices (250 µm) were cut, transferred in culture medium (Dulbecco's modified Eagle's medium containing 17% medium

Table 1 Different injection schedules for different peptide-PMO conjugates

Peptide conjugates	Dose	Age of animals	Number of injection	Time to harvest tissues after injection
Pip5e and B-PMO	25 mg/kg	2-month-old	Single	2 weeks
Pip5e and B-PMO	18.75 mg/kg	2-month-old	Single	2 weeks
Pip5e and B-PMO	18.75 mg/kg	6-month-old	Single	2 weeks
Pip5e and B-PMO	12.5 mg/kg	2-month-old	Single	2 weeks
Pip5j and Pip5l-PMO	25 mg/kg	2-month-old	Single	2 weeks

Abbreviation: PMO, phosphorodiamidate morpholino.

199, 10% horse serum, 5% fetal calf serum and 1% antibiotics) and incubated with Hoechst (to label nuclei) and fluorescently labeled (fluorescein isothiocyanate) Pip5e-PMO or B-PMO, or with Hoechst alone. After 10-minute incubation, live slices were imaged with a TCS-MP2 multi photon microscope (Leica Microsystems, Wetzlar, Germany) using 730 and 840 nm excitation wavelengths for nuclei and peptide-PMO conjugates, respectively. Colocalization of fluorescein isothiocyanate fluorescence within nuclei was measured using Image J. For RT-PCR measurements, slices were incubated with the peptide-PMO conjugate for 4 hours and kept in culture for at least 24 hours. RNA extraction and subsequent RT-PCR were carried out as described previously.[13]

Statistical analysis. All data are reported as mean values ± SEM. Statistical differences between treatment groups and control groups were evaluated by SigmaStat (Systat Software, London, UK) and the Student's *t*-test was applied.

SUPPLEMENTARY MATERIAL

Figure S1. Purification and analysis of Pip5e-PMO.
Figure S2. Clinical biochemistry and histological/immunological measures of systemic toxicity in *mdx* mice treated with either Pip5e-PMO or B-PMO conjugates at the 25 mg/kg dose.
Figure S3. Systemic dystrophin exon skipping induced by Pip5e-PMO at low doses of 18.75 mg/kg in adult and aged *mdx* mice.
Figure S4. Systemic evaluation of Pip5e-PMO in adult *mdx* mice at lower dose of 12.5 mg/kg.
Materials and Methods.

ACKNOWLEDGMENTS

This work was supported by research grants from the Muscular Dystrophy Campaign UK and Action Duchenne to M.J.A.W., MRC Unit program U105178803 and MRC-Technology Development Gap Fund support to M.J.G and National Natural Science Funding of China (No.81071443) and Chinese National Basic Research Program (973) (No.2011CB933104) to H.F.Y. The heart slice work was supported by the Oxford University EP Abraham Cephalosporin Fund to P.C. The authors acknowledge Professor Kay Davies (Department of Physiology, Anatomy and Genetics, University of Oxford, Oxford, UK) for providing access to facilities including the *mdx* mouse colony; Dr Hough (Clinical Pathology Laboratory, Mary Lyon Centre, MRC, Harwell, UK) for assistance with the clinical biochemistry assays; Christine Simpson for histological assays (Department of Physiology, Anatomy and Genetics, University of Oxford); and Alexandra Bussek (TU, Dresden, Germany) for training in the slice technique.

REFERENCES

1. Wood, MJ, Gait, MJ and Yin, H (2010). RNA-targeted splice-correction therapy for neuromuscular disease. *Brain* **133**(Pt 4): 957–972.
2. Wood, MJ (2010). Toward an oligonucleotide therapy for Duchenne muscular dystrophy: a complex development challenge. *Sci Transl Med* **2**: 25ps15.
3. Aartsma-Rus, A, Kaman, WE, Bremmer-Bout, M, Janson, AA, den Dunnen, JT, van Ommen, GJ *et al.* (2004). Comparative analysis of antisense oligonucleotide analogs for targeted DMD exon 46 skipping in muscle cells. *Gene Ther* **11**: 1391–1398.
4. Aartsma-Rus, A, Janson, AA, Kaman, WE, Bremmer-Bout, M, den Dunnen, JT, Baas, F *et al.* (2003). Therapeutic antisense-induced exon skipping in cultured muscle cells from six different DMD patients. *Hum Mol Genet* **12**: 907–914.
5. Aartsma-Rus, A, Janson, AA, Heemskerk, JA, De Winter, CL, Van Ommen, GJ and Van Deutekom, JC (2006). Therapeutic modulation of DMD splicing by blocking exonic splicing enhancer sites with antisense oligonucleotides. *Ann N Y Acad Sci* **1082**: 74–76.
6. Alter, J, Lou, F, Rabinowitz, A, Yin, H, Rosenfeld, J, Wilton, SD *et al.* (2006). Systemic delivery of morpholino oligonucleotide restores dystrophin expression bodywide and improves dystrophic pathology. *Nat Med* **12**: 175–177.
7. Gebski, BL, Mann, CJ, Fletcher, S and Wilton, SD (2003). Morpholino antisense oligonucleotide induced dystrophin exon 23 skipping in mdx mouse muscle. *Hum Mol Genet* **12**: 1801–1811.
8. Lu, QL, Mann, CJ, Lou, F, Bou-Gharios, G, Morris, GE, Xue, SA *et al.* (2003). Functional amounts of dystrophin produced by skipping the mutated exon in the mdx dystrophic mouse. *Nat Med* **9**: 1009–1014.
9. Mann, CJ, Honeyman, K, Cheng, AJ, Ly, T, Lloyd, F, Fletcher, S *et al.* (2001). Antisense-induced exon skipping and synthesis of dystrophin in the mdx mouse. *Proc Natl Acad Sci USA* **98**: 42–47.
10. van Deutekom, JC, Janson, AA, Ginjaar, IB, Frankhuizen, WS, Aartsma-Rus, A, Bremmer-Bout, M *et al.* (2007). Local dystrophin restoration with antisense oligonucleotide PRO051. *N Engl J Med* **357**: 2677–2686.
11. Wilton, SD, Fall, AM, Harding, PL, McClorey, G, Coleman, C and Fletcher, S (2007). Antisense oligonucleotide-induced exon skipping across the human dystrophin gene transcript. *Mol Ther* **15**: 1288–1296.
12. Yin, H, Lu, Q and Wood, M (2008). Effective exon skipping and restoration of dystrophin expression by peptide nucleic acid antisense oligonucleotides in mdx mice. *Mol Ther* **16**: 38–45.
13. Yin, H, Moulton, HM, Seow, Y, Boyd, C, Boutilier, J, Iverson, P *et al.* (2008). Cell-penetrating peptide-conjugated antisense oligonucleotides restore systemic muscle and cardiac dystrophin expression and function. *Hum Mol Genet* **17**: 3909–3918.
14. Yin, H, Moulton, HM, Betts, C, Seow, Y, Boutilier, J, Iverson, PL *et al.* (2009). A fusion peptide directs enhanced systemic dystrophin exon skipping and functional restoration in dystrophin-deficient mdx mice. *Hum Mol Genet* **18**: 4405–4414.
15. Wang, Q, Yin, H, Camelliti, P, Betts, C, Moulton, H, Lee, H *et al.* (2010). *In vitro* evaluation of novel antisense oligonucleotides is predictive of *in vivo* exon skipping activity for Duchenne muscular dystrophy. *J Gene Med* **12**: 354–364.
16. England, SB, Nicholson, LV, Johnson, MA, Forrest, SM, Love, DR, Zubrzycka-Gaarn, EE *et al.* (1990). Very mild muscular dystrophy associated with the deletion of 46% of dystrophin. *Nature* **343**: 180–182.
17. Gregorevic, P, Blankinship, MJ, Allen, JM, Crawford, RW, Meuse, L, Miller, DG *et al.* (2004). Systemic delivery of genes to striated muscles using adeno-associated viral vectors. *Nat Med* **10**: 828–834.
18. Kinali, M, Arechavala-Gomeza, V, Feng, L, Cirak, S, Hunt, D, Adkin, C *et al.* (2009). Local restoration of dystrophin expression with the morpholino oligomer AVI-4658 in Duchenne muscular dystrophy: a single-blind, placebo-controlled, dose-escalation, proof-of-concept study. *Lancet Neurol* **8**: 918–928.
19. Jearawiriyapaisarn, N, Moulton, HM, Buckley, B, Roberts, J, Sazani, P, Fucharoen, S *et al.* (2008). Sustained dystrophin expression induced by peptide-conjugated morpholino oligomers in the muscles of mdx mice. *Mol Ther* **16**: 1624–1629.
20. Wu, B, Moulton, HM, Iversen, PL, Jiang, J, Li, J, Li, J *et al.* (2008). Effective rescue of dystrophin improves cardiac function in dystrophin-deficient mice by a modified morpholino oligomer. *Proc Natl Acad Sci USA* **105**: 14814–14819.
21. Yin, H, Moulton, HM, Betts, C, Merritt, T, Seow, Y, Ashraf, S *et al.* (2010). Functional rescue of dystrophin-deficient mdx mice by a chimeric peptide-PMO. *Mol Ther* **18**: 1822–1829.
22. Ivanova, GD, Arzumanov, A, Abes, R, Yin, H, Wood, MJ, Lebleu, B *et al.* (2008). Improved cell-penetrating peptide-PNA conjugates for splicing redirection in HeLa cells and exon skipping in mdx mouse muscle. *Nucleic Acids Res* **36**: 6418–6428.
23. Yin, H, Betts, C, Saleh, AF, Ivanova, GD, Lee, H, Seow, Y *et al.* (2010). Optimization of peptide nucleic acid antisense oligonucleotides for local and systemic dystrophin splice correction in the mdx mouse. *Mol Ther* **18**: 819–827.
24. Brenman, JE, Chao, DS, Gee, SH, McGee, AW, Craven, SE, Santillano, DR *et al.* (1996). Interaction of nitric oxide synthase with the postsynaptic density protein PSD-95 and alpha1-syntrophin mediated by PDZ domains. *Cell* **84**: 757–767.
25. Newey, SE, Benson, MA, Ponting, CP, Davies, KE and Blake, DJ (2000). Alternative splicing of dystrobrevin regulates the stoichiometry of syntrophin binding to the dystrophin protein complex. *Curr Biol* **10**: 1295–1298.
26. Glesby, MJ, Rosenmann, E, Nylen, EG and Wrogemann, K (1988). Serum CK, calcium, magnesium, and oxidative phosphorylation in mdx mouse muscular dystrophy. *Muscle Nerve* **11**: 852–856.
27. Koshelev, M, Sarma, S, Price, RE, Wehrens, XH and Cooper, TA (2010). Heart-specific overexpression of CUGBP1 reproduces functional and molecular abnormalities of myotonic dystrophy type 1. *Hum Mol Genet* **19**: 1066–1075.
28. Wang, GS, Kuyumcu-Martinez, MN, Sarma, S, Mathur, N, Wehrens, XH and Cooper, TA (2009). PKC inhibition ameliorates the cardiac phenotype in a mouse model of myotonic dystrophy type 1. *J Clin Invest* **119**: 3797–3806.
29. Wu, B, Lu, P, Benrashid, E, Malik, S, Ashar, J, Doran, TJ *et al.* (2010). Dose-dependent restoration of dystrophin expression in cardiac muscle of dystrophic mice by systemically delivered morpholino. *Gene Ther* **17**: 132–140.
30. Alter, J, Sennoga, CA, Lopes, DM, Eckersley, RJ and Wells, DJ (2009). Microbubble stability is a major determinant of the efficiency of ultrasound and microbubble mediated *in vivo* gene transfer. *Ultrasound Med Biol* **35**: 976–984.
31. Tomonari, K (1988). A rat antibody against a structure functionally related to the mouse T-cell receptor/T3 complex. *Immunogenetics* **28**: 455–458.
32. Bussek, A, Wettwer, E, Christ, T, Lohmann, H, Camelliti, P and Ravens, U (2009). Tissue slices from adult mammalian hearts as a model for pharmacological drug testing. *Cell Physiol Biochem* **24**: 527–536.